https://doi.org/10.5194/egusphere-2026-3732
Preprint. Discussion started: 14 July 2026

Portable system for characterizing greenhouse gas analyzers for sensitivity to water vapor

Yunsong Liu[1], Natasha L. Miles[1], Scott J. Richardson[1], David O. Miller[2]

[1]Department of Meteorology and Atmospheric Science, The Pennsylvania State University, University Park, PA, 16802, USA
[2]Applied Research Laboratory, The Pennsylvania State University, University Park, PA, 16802, USA

Correspondence to: Yunsong Liu (yzl6376@psu.edu)

Abstract. Water vapor introduces dilution, spectral interference and pressure-broadening effects in greenhouse gas (GHG) measurements using infrared (IR) techniques. Accurate water vapor corrections are therefore required for measurements of ambient air samples that are undried or incompletely dried as is the case for commonly used permeation water exchangers. In this study, we developed a lightweight, low-cost, and portable system for performing water vapor corrections of GHG analyzers in both laboratory and field environments. The system uses a permeable membrane-based moisture exchanger (Permapure, Inc., BE series) to humidify gas from a compressed cylinder with known analyte mole fractions. This humidified stream is mixed with a parallel dry stream from the same cylinder to produce air with controlled water vapor levels. Water-vapor (H_2O) concentrations are held constant for a defined interval and then stepped across a range of user-defined levels. Gas flow rates are regulated using mass flow controllers, and a Raspberry Pi-based Linux system automates the sequence of water vapor steps and records measurement data for subsequent analysis. Compared to previously available dew point generators, the system provides substantially improved water vapor stability (approximately 3 ppm H_2O). The system was used to characterize water vapor corrections for Aeris MIRA Ultra and Picarro cavity ring-down spectroscopy (CRDS) analyzers. The two tested Aeris MIRA Ultra analyzers exhibited quadratic relationships for methane (CH_4), with distinct behaviors observed between low- and high-H_2O regimes, with errors of up to 30 ppb CH_4 at 3% H_2O if uncorrected. However, these two tested Aeris MIRA Ultra analyzers did not show clear dependence on water vapor for ethane (C_2H_6). Across the investigated humidity range, all three tested Picarro analyzers showed a nearly linear dependence for carbon dioxide (CO_2), and both analyzers tested for CH_4 exhibited a similar near-linear response. For carbon monoxide (CO), however, two of the three tested analyzers displayed a quadratic humidity dependence, and one did not show any dependence on water vapor. For the Picarro analyzers, the errors if uncorrected for water vapor response were as large as 0.25 ppm CO_2, 2.0 ppb CH_4, and 12 ppb CO, all at 1.7% H_2O. After applying the derived analyzer-specific water vapor correction functions to all datasets, the corrected CH_4, CO_2, and CO measurements from Aeris MIRA Ultra and Picarro analyzers were well within the WMO/GAW inter-laboratory compatibility goals. These results demonstrate that the system provides a practical and reliable approach for conducting water vapor corrections for GHG analyzers in laboratory and field applications.

https://doi.org/10.5194/egusphere-2026-3732
Preprint. Discussion started: 14 July 2026

1 Introduction

Atmospheric greenhouse gases (GHGs) measurements are fundamental for understanding how natural processes and human activities influence the global carbon cycle and for quantifying the sources, sinks and temporal variability of these gases. High-precision observations provide critical constraints for inverse models of atmospheric GHG transport and enable detection of long-term trends, seasonal cycles, and spatial gradients. Since water vapor (H_2O) exhibits large variability across spatial and temporal scales and induces a strong dilution effect on GHG mole fractions, GHG measurements should be reported as dry air mole fractions (Zellweger et al., 2025). This is necessary to isolate true variability in GHG abundances and to ensure consistency and comparability across observations used in Earth system studies and emission assessments. Besides dilution effects, measurements of GHGs in air using infrared (IR) techniques, e.g. Cavity Ring-Down Spectroscopy (CRDS) and mid-infrared absorption (MIRA) analyzers, are also affected by water vapor through spectral interference and pressure-broadening effects (Filges et al., 2015; Karion et al., 2013; Liu et al., 2026).

A common mitigation strategy for minimizing water vapor interference in GHG measurements is to dry the air sample. However, even low residual water vapor (~1000 ppm) can introduce significant biases in applications requiring high compatibility (as defined by the World Meteorological Organization, WMO) across analyzers and sites. An alternative approach is to dry the sample air and humidify the calibration gases, thereby minimizing the water vapor effect to that associated with the remaining difference in water vapor mole fraction between the sample and calibration gases. However, this difference often still exceeds 500 ppm H_2O, potentially resulting in significant measurement errors. To further address the remaining error, analyzers can be calibrated with gas cylinders of known analyte mole fractions while introducing controlled amounts of water vapor. Such calibrations should be performed regularly to ensure long-term measurement stability and WMO compatibility. CRDS as implemented by Picarro Inc. has been extensively evaluated in both laboratory and field conditions by several research groups, and previous studies have demonstrated that water vapor dilution and spectroscopic effects on carbon dioxide (CO_2) and methane (CH_4) can be corrected with high precision (Chen et al., 2010; Hazan et al., 2016; Morgan et al., 2015; Rella et al., 2013).

Several approaches have been used to generate controlled humidity levels for calibration. Chen et al. (2010) and Rella et al. (2013) employed a Licor 610 dew point generator to produce water vapor levels at discrete steps of up to 6%. However, the minimum achievable level was 0.6 % (6000 ppm) and the precision was relatively large at 23 ppm (1σ) at 4% H_2O. The National Oceanic and Atmospheric Administration (NOAA) developed a gas-permeable membrane-based water calibration system (Rella et al., 2013) for H_2O ranging between 0.7% (7000 ppm) and 4.2% (42000 ppm) but with a large physical footprint only appropriate for laboratory use. A water droplet method described by Rella et al. (2013) produces continuously varying humidity, but it lacks discrete control and often results in abrupt changes of water vapor mole fractions, with sparse measurements in certain water vapor ranges. Reum et al. (2019) used dry and wet air streams using a gas washing bottle to directly humidify the wet stream, adjusting the proportions manually. This approach places the sample gas in direct contact with liquid water, and it can alter the delivered mole fractions of water-soluble gases such as CO_2 through dissolution and

https://doi.org/10.5194/egusphere-2026-3732
Preprint. Discussion started: 14 July 2026

outgassing effects. More recently, Liu et al. (2026) applied a membrane-based water exchanger to produce continuously varying water vapor levels for calibrating CH_4/C_2H_6 measurements. However, without discrete steps, it is difficult to distinguish analyzer noise from water vapor induced effects. As highlighted in Liu et al. (2026), this limitation is particularly significant for analyzers such as the MIRA Ultra developed by Aeris Technologies Inc., where separating noise from water vapor dependent biases remains challenging.

In this paper, we introduce a new portable and automated system that enables water-vapor calibrations to be performed directly in the field. This system is straightforward to operate and allows multiple calibrations to be completed in several hours, thereby improving calibration statistics during onsite testing. In addition, its compact design represents a significant advancement over existing approaches, as it is easily portable, automated, and capable of battery-powered operation. In Sect. 2, we describe the system design and methodology, along with its applications to water vapor dependence tests for two Aeris MIRA Ultra analyzers and three Picarro analyzers. For clarity, the corresponding results are also presented within this section. Finally, in Sect. 3, we discuss advantages of this system relative to previously published approaches and outline implications for future applications.

2 Methodology and Results

2.1 The Portable Water vapor Analyzer Verification and Evaluation System (P-WAVES)

The system, called the Portable Water vapor Analyzer Verification and Evaluation System (P-WAVES), splits air from a cylinder of compressed calibration gas into two streams: an unmodified dry air stream and a humidified (wet) air stream (Fig. 1). A control valve (Clippard, ES-2W-12-L) is used to stop the gas flow from the calibration cylinder in between tests. The air is split using a tee with mass flow controllers (Alicat, Inc., MC-200SCCM-D-DB9M/5M, RIN, 5IN, GAS: AIR) arranged in parallel to independently regulate the flow rates of the wet and dry calibration gas. The wet branch of air is produced by passing through a membrane-based moisture exchanger (Perma Pure LLC: BE-060-24COMP2-SS) submersed in distilled or de-ionized water. A glass jar was used for the water vessel in these tests. The resulting saturated wet air stream is then combined with the dry air using a tee to produce a mixed gas flow with the desired water vapor mole fraction, which is then delivered to the test analyzer. This method creates stable water vapor levels (limited by the stability of the water bath temperature) up to the saturation vapor pressure of the ambient conditions (approximately 3%/30,000 ppm H_2O at 24°C).

The entire system is housed within a portable enclosure (30.5 cm × 30.5 cm × 20.3 cm) with a total system weight of less than 5 kg. The enclosure integrates a power supply (Traco Power, Inc., TPP 65-321M2) to provide electrical power to the mass flow controllers, the valves, and a Raspberry Pi (Model 4B). The Raspberry Pi-based control system with custom Python operating code automates the operation of the unit. Serial data from the test system to be calibrated (in this case, an Aeris MIRA Ultra analyzer or a Picarro analyzer) is ingested by the Raspberry Pi via a Universal Serial Bus (USB) connection and combined with ancillary data from the P-WAVES. The user inputs the desired calibration range (up to a maximum determined

https://doi.org/10.5194/egusphere-2026-3732
Preprint. Discussion started: 14 July 2026

from the measured water bath temperature), the number of discrete steps over the range, and the duration at each step. Low power requirements make a battery-operated version feasible.

The Python control software regulates the flow rates of the dry and humidified air streams and controls the duration for each water vapor step. Through automated adjustment of these parameters, the system generates a sequence of discrete water vapor mole fraction levels with user-defined time intervals. The system is currently configured to operate in either a monotonically increasing step sequence or a sequence that increases and then decreases. The latter approach enables evaluation of hysteresis effects and may help differentiate whether system noise or drift is the predominant error during a calibration test, but also requires longer steps to allow for drying the system. Alternative sampling patterns can be implemented through minor modifications to the control software.

To achieve very low water vapor mole fractions (< ~200 ppm), a three-way valve is installed just before the tee that recombines the wet and dry streams. To achieve the driest possible sample, the valve actuates and closes off the wet side. Without this valve, and even though no air is going through the wet branch, diffusive mixing at the wet/dry tee prevents a totally dry air stream. In addition, when the three-way valve is actuated, the system is programmed to vent a small amount (~ 5 ccm) of wet air to ambient, thereby maintaining equilibrium within the moisture exchanger. While a simple shutoff valve could be used in place of the three-way valve, it would not preserve this equilibrium condition. Following completion of a test with the water vapor unit, a second three-way valve located downstream of the moisture exchanger is activated to direct dry air through the wet side of the system to prevent condensation while the unit is not in use.

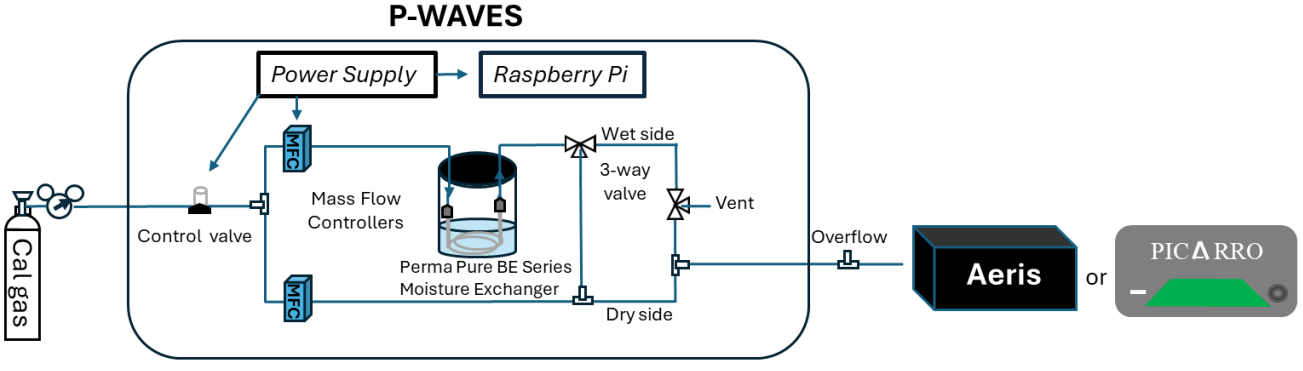

Figure 1: Schematic of the system (P-WAVES).

As an example of the operation of the system, the system was connected to an Aeris MIRA Ultra analyzer (serial number A778). In this configuration, each water vapor step was maintained for a duration of 3.5 minutes (Fig. 2), with steps up to 0.7% H_2O. The stability of the water vapor during the last 60 s of each step was 1.2 ± 0.4 ppm H_2O, indicating stable and repeatable humidity control suitable for water vapor sensitivity testing of greenhouse gas measurements.

https://doi.org/10.5194/egusphere-2026-3732
Preprint. Discussion started: 14 July 2026

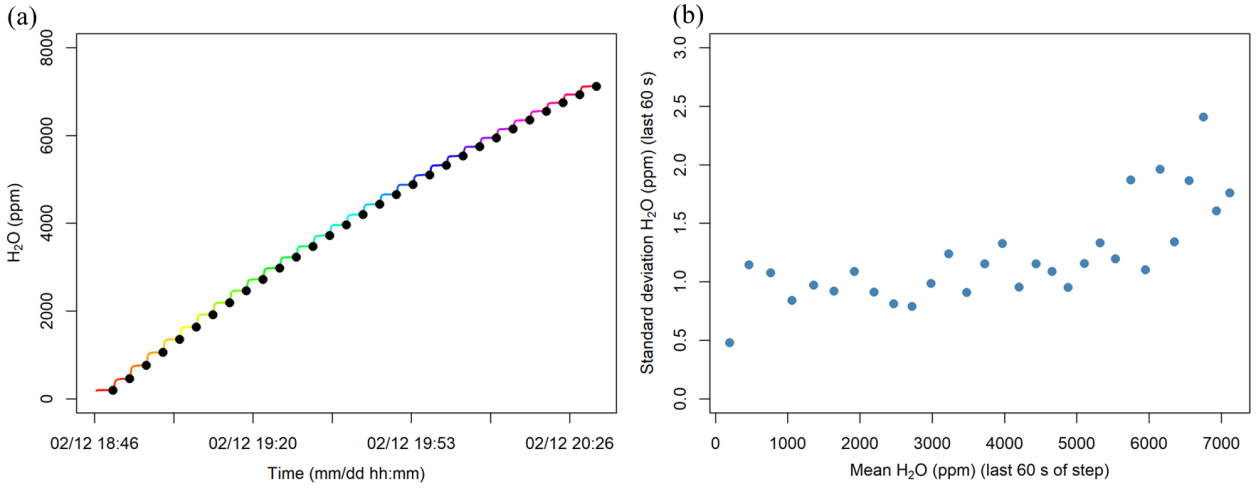

Figure 2: (a) Time series of water vapor controlled by P-WAVES. Individual raw data are shown in a different color for each step and the mean over the last 60 s of each step is indicated by black dots. (b) Precision (1-σ) of water vapor mole fractions during the last 60 s of each step, as a function of mean water vapor mole fraction.

2.2 Water vapor correction of greenhouse gas measurements

For near- and mid-infrared analyzers, water vapor affects measured GHG mole fractions through spectral interference, pressure-broadening, and dilution effects, which can be corrected using analyzer-specific quadratic functions based on measured H_2O mole fractions. Here, water vapor correction functions were characterized for each species X following established approaches (e.g. Chen et al., 2010; Morgan et al., 2015; Hazan et al., 2016; Rella et al., 2013). The correction was parameterized as a second-order quadratic function of the measured water vapor mole fraction, expressed as:

$$\frac{X_{wet}}{X_{dry}} = 1 + a \times H_2O_{rep} + b \times H_2O_{rep}^2 \qquad \text{Eq. (1)}$$

Here H_2O_{rep} represents the water vapor mole fraction measured by the test analyzer, while a and b are empirically derived coefficients obtained from dedicated water vapor correction experiments. In this study, uncorrected (wet) mole fractions measured by the test analyzers were used directly, and the corresponding dry mole fractions were defined as the assigned value of the calibrated gas cylinder (i.e., a constant). An offset correction was applied to each test to account for instrument noise between tests.

Water vapor correction functions were characterized for two Aeris MIRA Ultra analyzers (series number A778 and A798) for CH_4 and C_2H_6, and for three Picarro analyzers (CFKADS2218, CFKADS2025, and CKADS2025) for CO_2, CO, and where available CH_4 (CFKADS2218 and CFKADS2025), using the P-WAVES system. (Note the unfortunate similarity in the serial numbers between CFKADS2025 and CKADS2025). A calibrated cylinder with known CO_2 (432.8 ppm) and CH_4 (2025.0 ppb) was used during the experiments, traceable to the WMO CO_2 scale (WMO-CO2-X2019) and CH_4 scale (WMO X2004A), respectively. For species without certified cylinder values (i.e., CO), the dry mole fraction was determined as the value

https://doi.org/10.5194/egusphere-2026-3732
Preprint. Discussion started: 14 July 2026

measured by the test analyzer under near-dry conditions (H_2O < 100 ppm). For ethane, the value of the calibration cylinder was estimated to be about 1.5 ppb.

During the experiments, each water vapor step was maintained for 3-5 min and only the last 60 s of data (representing stable conditions) were used to derive the correction functions. When using permeation water exchangers (e.g. Nafion) to dry the sample stream for instruments deployed in the field, the residual H_2O content is typically below 2000 ppm (Liu et al., 2026) so additional tests in this water vapor range were conducted. As measured by the Aeris analyzer, the differences in water vapor mole fraction between the dried sample and the humidified calibration gas in the field are generally in the range of 100-500 ppm (Liu et al., 2026). In this study, the water vapor correction experiment was repeated 4 times per analyzer with water vapor mole fraction below 2000 ppm (low H_2O tests; denoted as L1, L2, …) and 4-6 times up to approximately 30000 ppm (3%) for Aeris MIRA Ultra analyzers (Saturation tests, denoted as S1, S2, …). For Picarro analyzers, the experiment was repeated 4-5 times per analyzer with water vapor mole fraction up to approximately 17000 ppm (1.7%). The lower maximum water vapor levels for the Picarro analyzers (with higher flow rates than the Aeris analyzers) was due to a limitation of the mass flow controllers used in this version of the water calibration system; the use of different mass flow controllers would allow testing up to the saturation for the Picarro analyzers. To assess the stability of the fitted coefficients *a* and *b*, the relative stability (RS) was defined as the ratio of the standard deviation to the absolute mean value for each coefficient. Smaller RS values indicate higher stability. Detailed results of these tests are presented in the following sections.

2.2.1 Aeris MIRA Ultra analyzers

The uncorrected (wet) methane mole fraction reported by the Aeris analyzers exhibited substantial and analyzer-dependent sensitivity to water vapor, with distinct behavior observed at water vapor mole fractions below 3000 ppm (Fig. S1). For both analyzers, repeatable but analyzer-specific quadratic relationships were observed for tests spanning water vapor mole fractions up to saturation (about 30000 ppm), and these relationships remained stable over an interval of approximately one month (Fig. 3, Table 1, and Fig. S1). The fits for the tests up to saturation were relatively stable, with RS values of 1-2% (Table 1). The residual errors of the quadratic fits for the full range up to 30000 ppm H_2O were below 1.5 ppb CH_4 for analyzer serial number A778 (Fig. 3). A second-order quadratic fit did not fully capture the dependence on water vapor at low humidity levels for tests up to saturation for A798, leading to residuals up to 6.0 ppb CH_4. Applying separate fits using the tests below 3000 ppm H_2O reduced the residual errors to approximately 0.3 ppb for analyzer A778 and 1.5 ppb for analyzer A798 (Fig. 3b,d). Another option to improve the residuals is to apply a third-order polynomial fit, reducing the error to 1.5 ppb for analyzer A798 for the full range up to 30000 ppm H_2O. The uncorrected (wet) methane exhibited little dependence on water vapor in the low water vapor range, less than 3 ppb CH_4 (Fig. S1a,c), and thus the coefficients of these quadratic fits at low H_2O exhibited variability over repeated tests for both analyzers (with RS ranging from 68% to 182%) (Table 1).

https://doi.org/10.5194/egusphere-2026-3732
Preprint. Discussion started: 14 July 2026

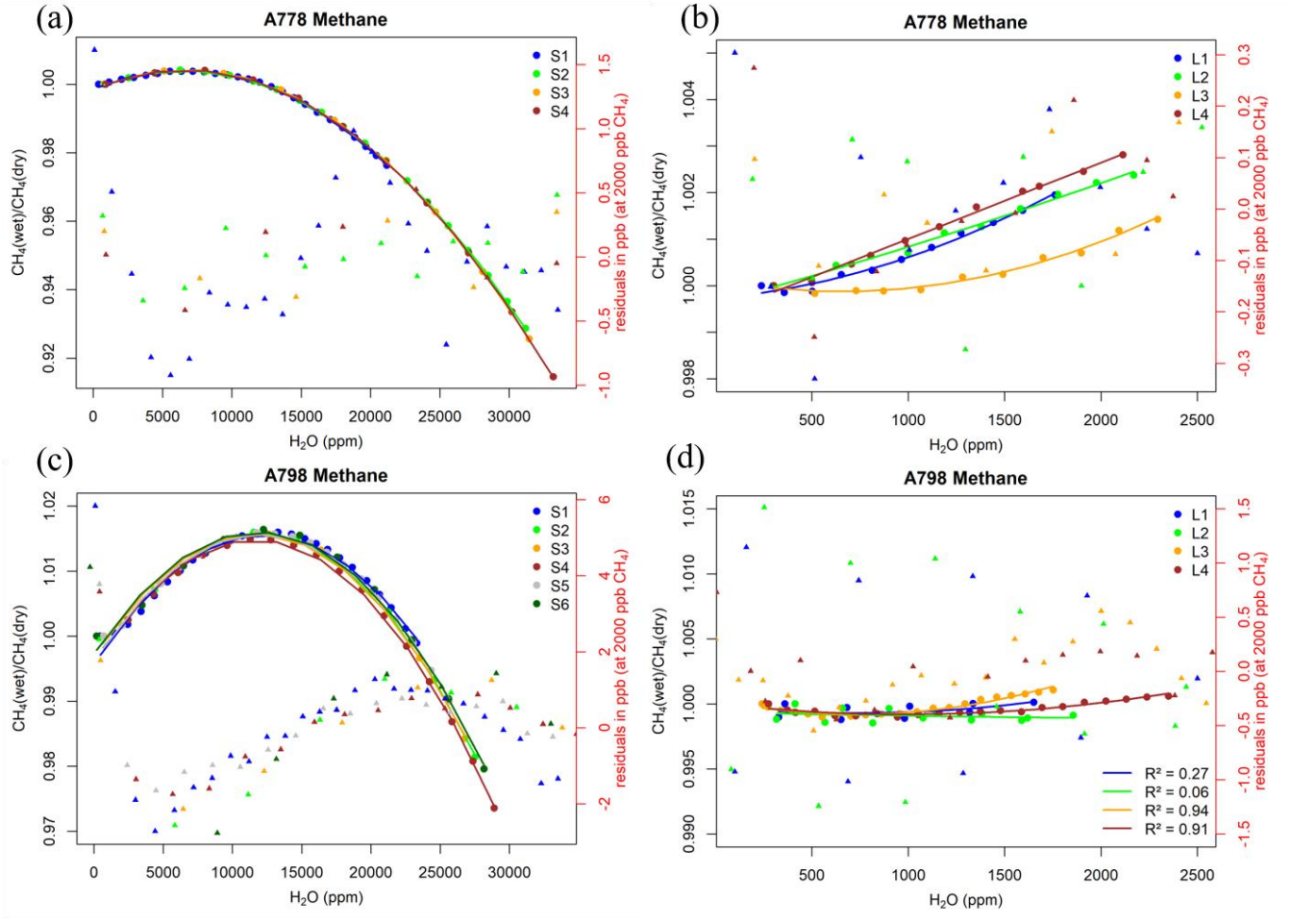

Figure 3: Quadratic fits of CH_4(wet)/CH_4(dry) as a function of H_2O mole fraction for the serial numbers A778 and A798. (a) and (c) show saturation tests (S1-S4 for A778 and S1-S6 for A798). (b) and (d) show low H_2O tests (L1-L4) for A778 and A798 respectively. Solid lines represent the corresponding quadratic fits for each test. Triangle symbols in (a–d) represent residuals of corresponding fits, with colors indicating different tests, and residuals are read on the axis to the right. Here CH_4(dry) is the known value of the cylinder, 2025.0 ppb. An offset correction was applied. Coefficients of determination (R^2) lower than 0.99 are shown in panel (d), and fits with $R^2 \geq 0.99$ are not labeled for clarity.

Table 1: A summary of the test results for the serial number A778 and A798. Note: N/A indicates not available. RS denotes relative stability (defined in Section 2.2). Residuals reported in this table are calculated after applying the experimentally determined water vapor correction.

https://doi.org/10.5194/egusphere-2026-3732
Preprint. Discussion started: 14 July 2026

H_2O Range	Serial Number	Test No.	Date (2026)	CH_4 $a\times10^{-6}$	CH_4 $b\times10^{-10}$	R^2	Residual error at 2000 ppb CH_4 (at 500 ppm H_2O)	Residual error at 2000 ppb CH_4 (at 1% H_2O)
Up to ~30000 ppm (3%)	A778	S1	Mar 19	1.67	-1.28	1	1.61	0.24
		S2	Apr 13	1.63	-1.24	1	0.32	-0.02
		S3	Apr 13	1.71	-1.28	1	0.20	-0.31
		S4	Apr 13	1.69	-1.27	1	0.02	0.23
		Mean ± SD (RS%)		1.67±0.04 (2%)	-1.27±0.02 (1%)	N/A	0.54±0.63	0.04±0.22
	A798	S1	Mar 17	3.25	-1.32	0.98	5.83	0.30
		S2	Apr 14	3.24	-1.38	1	2.32	0.20
		S3	Apr 14	3.2	-1.37	1	1.77	0.13
		S4	Apr 14	3.21	-1.38	1	3.58	0.15
		S5	Apr 14	3.27	-1.36	0.99	3.77	-0.21
		S6	Apr 14	3.17	-1.34	0.99	4.22	-0.82
		Mean ± SD (RS%)		3.22±0.04 (1%)	-1.36±0.02 (2%)	N/A	3.58±1.31	-0.04±0.38

H_2O Range	Serial number	Test No.	Date (2026)	CH_4 $a\times10^{-6}$	CH_4 $b\times10^{-10}$	R^2	Residual error at 2000 ppb CH_4 (at 500 ppm H_2O)
< 3000 ppm (0.3%)	A778	L1	Mar 19	0.35	5.29	0.99	-0.33
		L2	Mar 19	1.13	0.77	0.99	-0.14
		L3	Mar 19	-0.79	5.97	0.99	-0.11
		L4	Mar 19	1.63	0.03	0.99	-0.25
		Mean ± SD (RS%)		0.58±1.06 (182%)	3.02±3.05 (101%)	N/A	-0.21±0.09
	A798	L1	Mar 16	-1.47	10.1	0.27	0.84
		L2	Mar 16	-0.31	0.4	0.06	1.51
		L3	Mar 18	-2.97	20.5	0.94	-0.55
		L4	Mar 18	-1.72	8.68	0.91	0.10
		Mean ± SD (RS%)		-1.62±1.09 (68%)	9.92±8.23 (83%)	N/A	0.48±0.77

For ethane, no clear dependence on water vapor was observed during the experiments (Fig. S1) for the uncorrected (wet) values. Manufacturer corrected values (not used here) were within 0.2 ppb C_2H_6 of the wet values for H_2O less than 2% (Fig. S2). Noise within and between tests was approximately 2 ppb C_2H_6, nearly an order of magnitude larger than the compatibility goal of 0.3 ppb (Liu et al., 2026). Noise appears to be the dominant factor for ethane, requiring the calibration procedures documented in Liu et al. (2026), depending on the application.

The methane mole fractions corrected using the analyzer-specific quadratic fits were more stable and showed smaller biases relative to the assigned methane mole fraction of the calibrated cylinder compared to the manufacturer-provided corrected (dry) methane values (Fig. 4). For analyzer A778, the bias of manufacturer-corrected methane reached approximately 30 ppb at water vapor mole fractions near 30000 ppm (3% H_2O), whereas the experimentally-derived correction yielded a bias below 0.5 ppb for H_2O mole fraction ranging from 0-30000 ppm (Fig. 4a). For tests conducted at H_2O mole fraction below 3000 ppm (Fig. 4b), the mean methane biases obtained using both the manufacturer-provided and the experimentally-derived correction were within the 3 ppb CH_4 target proposed by Liu et al. (2026) for tower-network measurements in basin regions, as well as within the WMO Global Atmosphere Watch (GAW) compatibility goal of ± 2 ppb CH_4 (Zellweger et al., 2025). In contrast, for analyzer A798, the bias of the manufacturer-corrected methane at high H_2O mole fractions was similar to that obtained using the experimentally-derived correction (Fig. 4c), while both corrections showed large bias (6-8 ppb CH_4) at low H_2O mole fractions using quadratic fits. For tests conducted at H_2O mole fractions below 3000 ppm (Fig. 4d), the manufacturer-corrected methane measurements exhibited a systematic water vapor dependent bias, decreasing with increasing H_2O mole

https://doi.org/10.5194/egusphere-2026-3732
Preprint. Discussion started: 14 July 2026

fraction and varying by about 10 ppb across the tested range. The bias at low water vapor values using the manufacturer correction (Fig. 4d) was thus worse than the uncorrected values (Fig. S1c). However, the bias was removed using the experimentally-derived correction, to below 1 ppb.

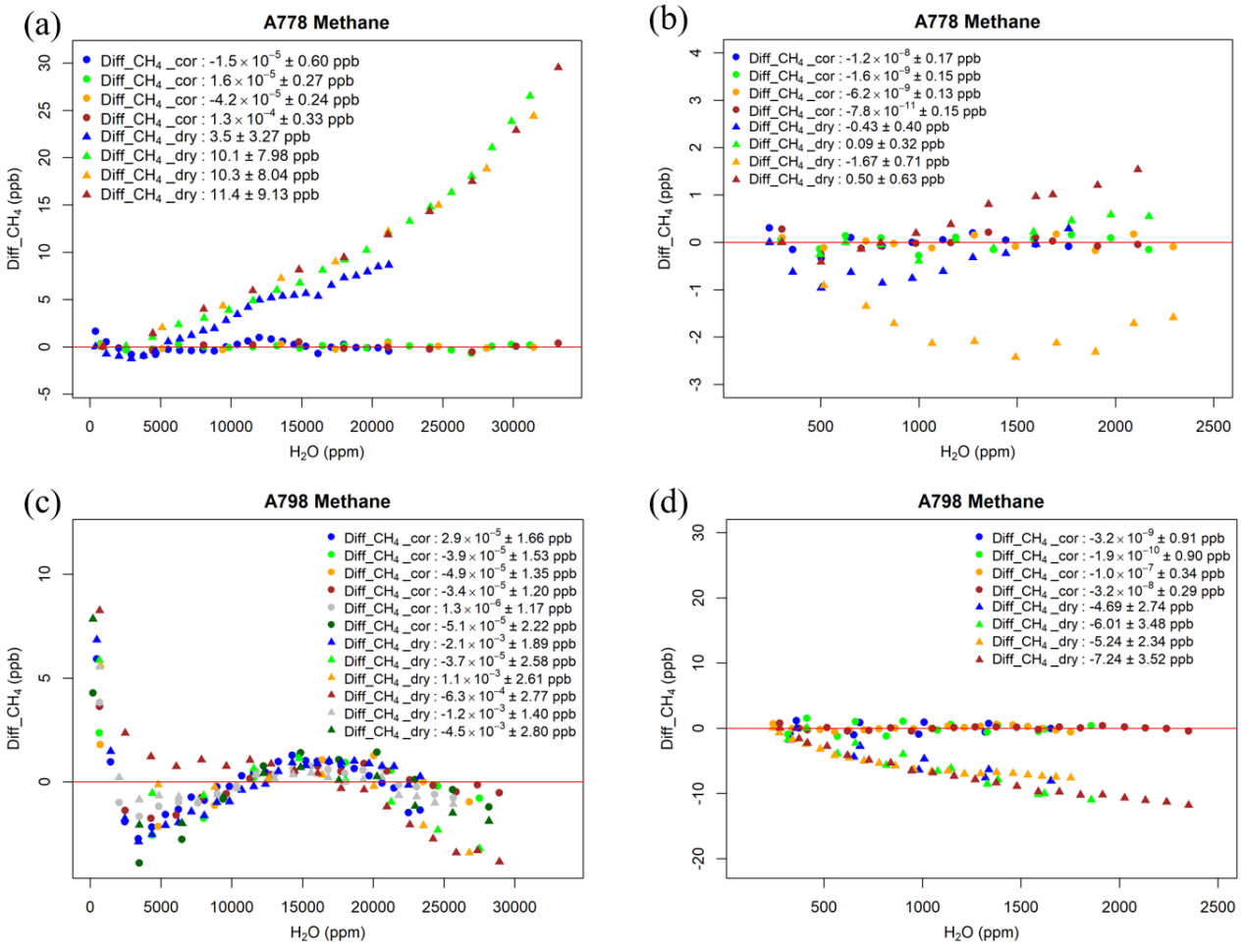

Figure 4: Methane bias as a function of H_2O mole fractions for the serial number A778 and A798. (a) and (c) show the saturation tests (S1-S4 for A778 and S1-S6 for A798). (b) and (d) show low H_2O tests (L1-L4) for A778 and A798 respectively. Circular symbols represent biases between methane values corrected using the corresponding quadratic fit and the assigned methane value of the calibrated cylinder, with colors indicating different tests. Triangle symbols represent biases between the manufacturer's corrected methane (dry) values and the assigned methane value of the calibrated cylinder, with colors indicating different tests. An offset correction was applied for each test. The red lines in (a–d) indicate zero bias. Values in the legends are the mean ± standard deviation for each test.

2.2.2 Picarro analyzers

Except for the CKADS2025 analyzer which did not exhibit a discernable water vapor effect for CO, the uncorrected (wet) mole fraction reported by the analyzers exhibited analyzer-specific water vapor correction functions for the measurands for water vapor mole fractions tested, up to about 17000 ppm (1.7% H_2O). The residual errors of the quadratic fits were below

https://doi.org/10.5194/egusphere-2026-3732
Preprint. Discussion started: 14 July 2026

0.02 ppm, 0.4 ppb and 3 ppb for CO_2, CH_4 and CO, respectively (Fig. 5-7). The quadratic fit for CO_2 and CH_4 was reproducible across experiments (Table 2), with RS for the coefficient *a* of 1% for CO_2 and 2-7% for CH_4. For CO, the RS for the coefficient *a* was 11-12% for CFKADS2025 and CFKADS2218, but large for CKADS2025 since there was no apparent water vapor dependence. For CO_2 and CH_4, the Picarro analyzers exhibit nearly linear response to water vapor, so the coefficient *b* is small and extremely variable (Table 2). Unlike the Aeris analyzers, there is no difference in the residuals at low versus high water vapor.

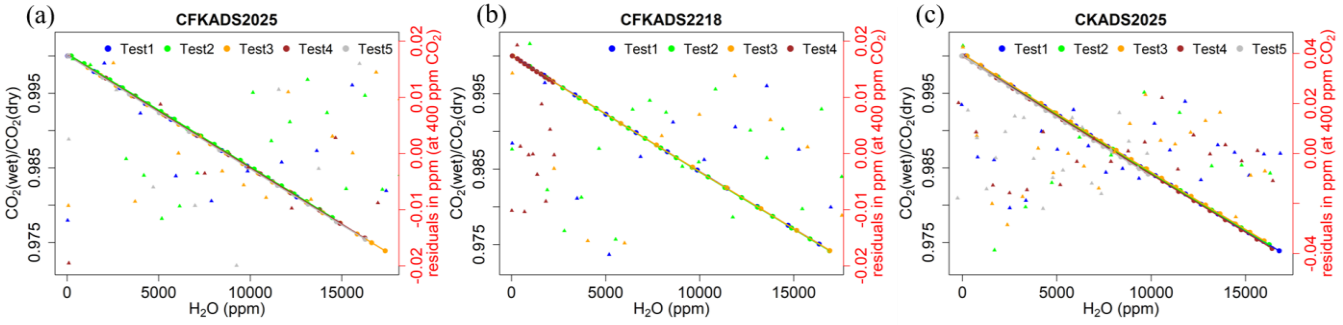

Figure 5: (a-c) Quadratic fits of CO_2(wet)/CO_2(dry) as a function of H_2O mole fraction for tested Picarro analyzers. Solid lines represent the corresponding quadratic fits for each test. Triangle symbols in (a–c) represent residuals of corresponding fits, with colors indicating different tests, and residuals are read on the axis to the right. Note that an offset correction was applied.

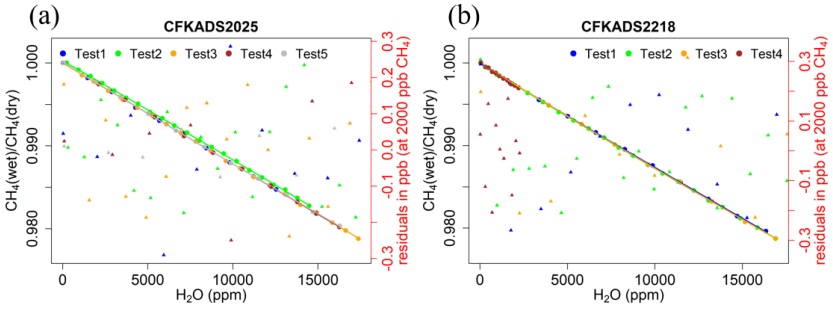

Figure 6: As for Fig. 5, but quadratic fits of CH_4(wet)/CH_4(dry) as a function of H_2O mole fraction for the tested Picarro analyzers measuring CH_4.

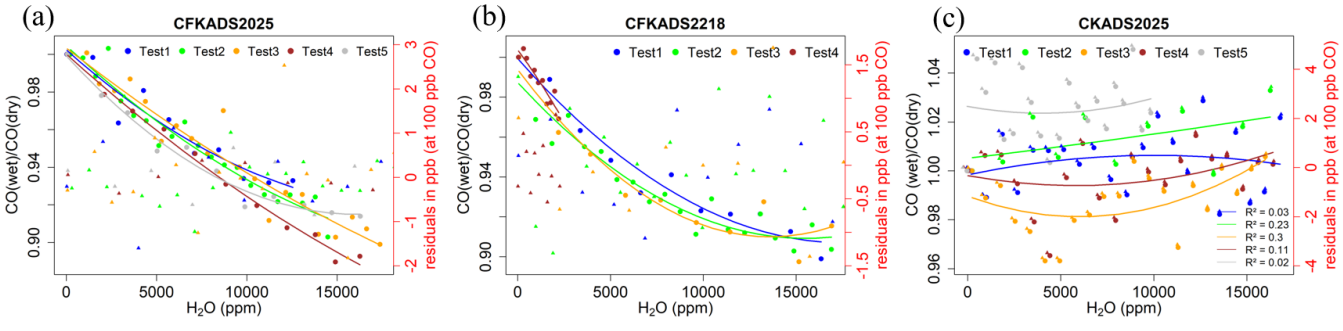

Figure 7: As for Fig. 5, but quadratic fits of CO(wet)/CO(dry) as a function of H_2O mole fraction for the tested Picarro analyzers.

https://doi.org/10.5194/egusphere-2026-3732
Preprint. Discussion started: 14 July 2026

Table 2: A summary of the test results for Picarro CFKADS2025, CFKADS2218 and CKADS2025. Note: N/A indicates not available. RS denotes relative stability (defined in Section 2.2). Residuals reported in this table are calculated after applying the experimentally determined water vapor correction. For CKADS2025, there was no dependence of CO(wet) on H_2O, so a=0 and b=0.

Picarro	Test No.	Date (2026)	CO_2		R^2	CH_4		R^2	CO		R^2	Residual error at 400 ppm CO_2 (at 500 ppm H_2O)	Residual error at 400 ppm CO_2 (at 1% H_2O)	Residual error at 2000 ppb CH_4 (at 500 ppm H_2O)	Residual error at 2000 ppb CH_4 (at 1% H_2O)	Residual error at 100 ppb CO (at 500 ppm H_2O)	Residual error at 100 ppb CO (at 1% H_2O)
			$a\times10^{-6}$	$b\times10^{-13}$		$a\times10^{-6}$	$b\times10^{-12}$		$a\times10^{-6}$	$b\times10^{-10}$							
CFKADS2025	1	Mar 5	-1.51	-3.93	1	-1.23	0.87	1	-8.57	2.19	0.91	0.01	0.001	0.05	-0.07	-0.21	-0.54
	2	Mar 25	-1.51	-1.49	1	-1.18	-1.81	1	-8.85	1.74	0.95	0.02	0.01	0.01	0.23	-0.25	-0.20
	3	Mar 25	-1.52	7.40	1	-1.22	0.27	1	-7.48	0.84	0.93	0.02	0.003	0.18	-0.24	-0.29	0.08
	4	Mar 25	-1.52	4.08	1	-1.24	1.03	1	-8.63	1.08	0.99	-0.02	0.003	0.02	0.13	0.06	-0.13
	5	Mar 27	-1.54	16.40	1	-1.25	1.90	1	-10.50	3.25	0.98	0.003	0.02	0.01	-0.07	0.15	-0.85
	Mean ± SD (RS%)		-1.52±0.01 (1%)	4.49±8.01 (179%)	N/A	-1.22±0.03 (2%)	0.45±1.39 (308%)	N/A	-8.80±1.08 (12%)	1.82±0.96 (53%)	N/A	0.01±0.02	0.01±0.01	0.05±0.06	-0.004±0.19	-0.11±0.20	-0.33±0.37
CFKADS2218	1	Mar 28	-1.56	18.7	1	-1.28	2.11	1	-10.5	2.98	0.96	0.002	-0.001	0.29	0.19	0.15	-0.18
	2	Mar 28	-1.57	21.5	1	-1.30	2.76	1	-10.1	3.25	0.92	0.001	-0.002	0.31	-0.13	1.32	1.14
	3	Mar 28	-1.56	15.4	1	-1.30	2.42	1	-12.3	4.53	0.92	0.01	0.01	0.20	0.31	0.71	0.03
	4	Mar 28	-1.60	-23.0	1	-1.47	33.10	1	-12.7	-7.06	0.86	0.001	N/A	0.16	N/A	0.20	N/A
	Mean ± SD (RS%)		-1.57±0.02 (1%)	8.13±20.91 (257%)	N/A	-1.34±0.09 (7%)	10.09±15.31 (152%)	N/A	-11.40±1.31 (11%)	0.92±5.34 (581%)	N/A	0.004±0.004	0.002±0.007	0.24±0.06	0.12±0.23	0.60±0.47	0.33±0.71

Picarro	Test No.	Date (2026)	CO_2		R^2	CO		R^2	Residual error at 400 ppm CO_2 (at 500 ppm H_2O)	Residual error at 400 ppm CO_2 (at 1% H_2O)	Residual error at 100 ppb CO (at 500 ppm H_2O)	Residual error at 100 ppb CO (at 1% H_2O)
			$a\times10^{-6}$	$b\times10^{-12}$		$a\times10^{-6}$	$b\times10^{-10}$					
CKADS2025	1	Mar 26	-1.64	3.93	1	1.60	-0.80	0.03	0.02	0.01	-1.09	2.23
	2	Mar 26	-1.64	4.20	1	0.92	0.07	0.23	0.04	0.02	0.36	2.43
	3	Mar 27	-1.61	2.93	1	-2.82	2.34	0.30	0.04	0.02	-1.12	-0.84
	4	Mar 27	-1.61	2.09	1	-1.41	1.21	0.11	0.02	0.02	0.63	-0.05
	5	Mar 27	-1.66	5.80	1	-1.39	1.73	0.02	0.02	-0.001	4.58	2.37
	Mean ± SD (RS%)		-1.63±0.02 (1%)	3.79±1.40 (37%)	N/A	-0.62±1.83 (294%)	0.91±1.27 (139%)	N/A	0.03±0.01	0.01±0.01	0.67±2.08	1.23±1.03

https://doi.org/10.5194/egusphere-2026-3732
Preprint. Discussion started: 14 July 2026

After applying the corresponding quadratic correction, the CO_2 and CH_4 mole fractions were more stable and showed reduced bias relative to the assigned cylinder values compared with the manufacturer-provided corrections (Figs. 8 and 9). The manufacturer-provided CO_2 correction (dry) resulted in residual biases of up to about 0.14-0.23 ppm, exceeding the WMO/GAW inter-laboratory compatibility goal for CO_2 (± 0.1 ppm in the Northern Hemisphere and ±0.05 ppm in the Southern Hemisphere) for all three analyzers, whereas the mean bias was eliminated using the experimentally-derived quadratic fits. The mean bias for CH_4 was just within the WMO/GAW compatibility goal of ± 2 ppb for the manufacturer-corrected data for CFKADS2025, CFKADS2218 and CKADS2025 analyzers, and eliminated using the experimentally-corrected fits (Fig. 9).

Picaro analyzers report only the uncorrected CO measurements and therefore, post-processing water vapor correction is necessary for high precision CO measurements. Without correction, CO biases reached about 12 ppb for CFKADS2025 and CFKADS2218 (Fig. 10). After applying the derived quadratic correction, the mean CO bias was reduced to 1 ppb, representing a substantial improvement. In contrast, CO measurements from CKADS2025 did not show a clear dependence on water vapor.

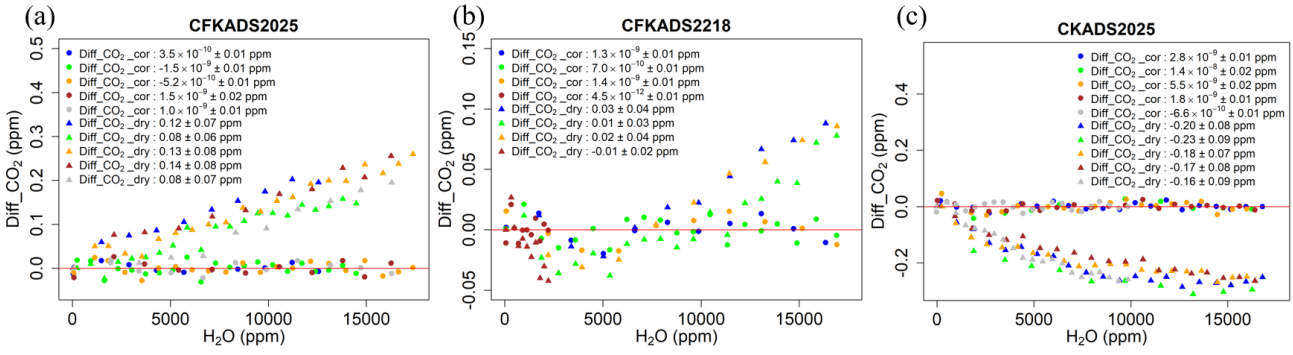

Figure 8: (a-c) The CO_2 bias as a function of H_2O mole fractions for Picarro analyzers CFKADS2025, CFKADS2218 and CKADS2025, respectively. Circular symbols represent biases between CO_2 values corrected using the corresponding quadratic fit and the assigned CO_2 value of the calibrated cylinder, with colors indicating different tests. Triangle symbols represent biases between the manufacturer's corrected CO_2 (dry) values and the assigned CO_2 value of the calibrated cylinder, with colors indicating different tests. The red lines in (a–c) indicate zero bias. Values in the legends are the mean ± standard deviation for each test. These tests lasted approximately 30-80 min, with 10-21 steps per test. Note that an offset correction was applied.

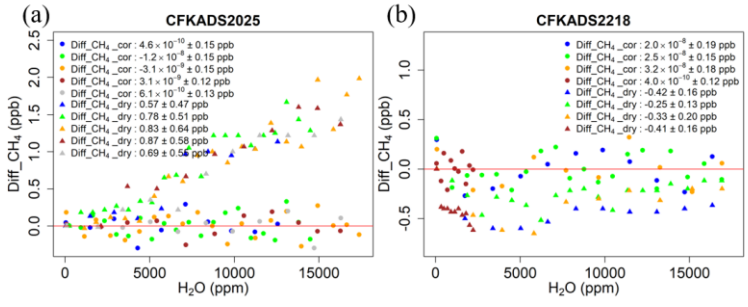

Figure 9: Same as for Fig. 8, but for CH_4 bias vs H_2O mole fractions for the Picarro analyzers measuring CH_4.

https://doi.org/10.5194/egusphere-2026-3732
Preprint. Discussion started: 14 July 2026

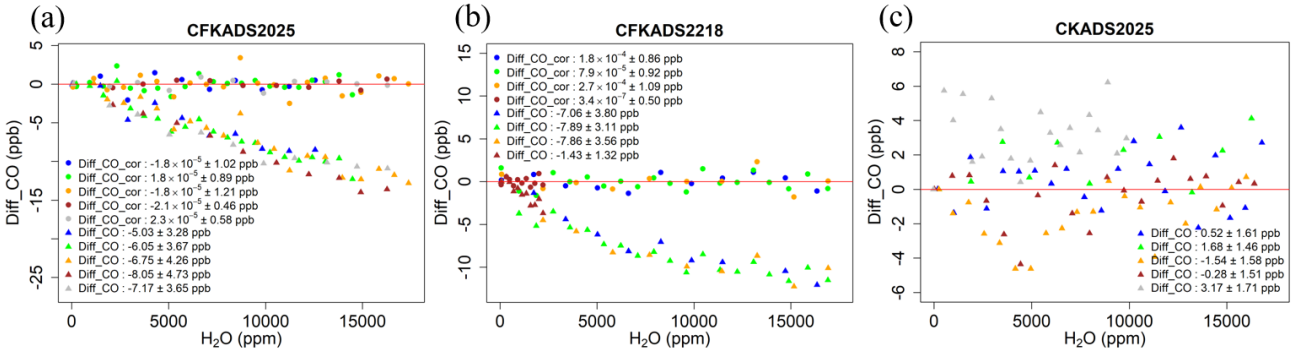

Figure 10: Same as for Fig. 8, but for CO bias vs. H_2O mole fraction for the tested Picarro analyzers.

3 Discussion and conclusions

Compared with commercially available dew point and humidity generators (e.g., Licor 610, Li-Cor Inc., USA) and previously published techniques (Chen et al., 2010; Rella et al., 2013; Reum et al., 2019) , the P-WAVES system developed in this study provides improved stability of water vapor mole fraction, while being smaller in size, lower in cost, and requiring less power. The lightweight and portable design makes the system straightforward to operate in a field setting. In addition, its relatively low cost makes the system easy to replicate and enables deployment of multiple units across GHG monitoring networks.

Potential future improvements to the P-WAVES system could further enhance humidity stability and expand the achievable operating range for specialized applications. Improvements could include replacing the glass water reservoir with a vacuum insulated container to improve thermal stability during extended experiments. Continuous monitoring of the water chamber temperature could also enable automated estimation of the maximum achievable water vapor mole fraction under varying environmental conditions. To achieve higher H_2O mole fractions for the Picarro analyzers, a different mass flow controller is needed. For applications requiring enhanced humidity stability or operation at elevated H_2O mole fractions, temperature stabilization of the enclosure and transfer lines could further improve performance and allow operation above ambient saturation levels, provided that all downstream components are sufficiently heated to prevent condensation. Although the Permapure BE series moisture exchanger used in this study provided stable operation without introducing liquid water or leak risks, alternative configurations using Permapure MH series humidifiers or MD series (gas driers but using a moist air stream as the purge flow) may also be used. However, such configurations may increase the risk of membrane seal failure, potentially resulting in leaks or introduction of liquid water into the system.

Several limitations of this study should be acknowledged. First, the number of analyzers tested was limited to three Picarro analyzers and two Aeris MIRA analyzers, and therefore the observed water vapor dependencies may not fully represent analyzer-to-analyzer variability across the broader analyzer population. Second, the tests were conducted over a limited time period (one month) and did not evaluate potential long-term temporal changes in the water vapor correction functions due to analyzer aging or instrumental drift. Third, although the dependence of CO_2 and CH_4 measurements on H_2O is nearly linear for the Picarro analyzers, if a dryer is not used in the field, these tests should ideally be conducted over the full range of

https://doi.org/10.5194/egusphere-2026-3732
Preprint. Discussion started: 14 July 2026

expected ambient water vapor mole fractions, up to the maximum anticipated value. The tested H_2O mole fraction range in this study was limited to approximately 1.7% for Picarro analyzers, and analyzer behavior at higher humidity levels up to 4% was not investigated. Additional studies including a larger number of instruments, longer-term characterization, and a broader humidity range would help further assess the robustness and general applicability of the derived correction relationships.

Previous studies have shown that CO_2 and CH_4 can permeate through Nafion membranes (Chiou and Paul, 1988; Naudy et al., 2014), with transport driven by partial pressure gradients between the sample streams. Welp et al. (2013) and Stavert et al. (2019) reported that such losses are generally small, typically below 0.05 ppm for CO_2 and 0.2 ppb for CH_4, well within the WMO/GAW compatibility goals. To further evaluate possible membrane exchange effects in this study, additional long-step tests were conducted using the CFKADS2025 analyzer with 30 min H_2O steps at 1% and 1.5%. The tests were repeated four times to assess repeatability. No detectable exchange was observed for CH_4 or CO under the tested conditions (not shown). For CO_2, small apparent drift rates ranging from approximately 0.04 to -0.12 ppm h^{-1} were observed among the repeated tests (Fig. S3). However, the magnitude and sign of the observed trends were not consistent between tests suggesting that these apparent changes were likely dominated by instrumental noise rather than systematic membrane permeation effects. Overall, the results indicate that any potential membrane exchange effect for CO_2 in the present setup was negligible under the tested conditions. In contrast to the approach described by Reum et al. (2019), the Nafion membrane-based humidification system used in this study humidifies the gas stream without direct gas-liquid contact, thereby minimizing solubility-related effects.

The results shown in this study have practical implications for the deployment and operational strategies of Aeris MIRA analyzers in atmospheric greenhouse measurement networks. Table 3 summarizes the advantages and disadvantages of various water vapor handling strategies for the Aeris MIRA analyzer measurements of CH_4 based on the results presented in this manuscript, assuming the analyzers evaluated here are broadly representative of similar analyzers. The relevant quantity is the difference between the water vapor of the sample air and the calibration gas and slopes in Fig. 4. One option is to not treat the sample air or calibration gas in terms of water vapor. In this case the errors are up to 30 ppb CH_4 if reliant on manufacturer water corrections, but this can be reduced to 6 ppb or less by experimentally developing analyzer specific corrections. For certain applications, for example, mobile measurements of large sources, this approach is reasonable. For others, this error is unacceptably large and treating the sample air and/or calibration gas is required. Drying the sample nearly completely (100 ppm H_2O) using a chiller and permeation water exchanger (Andrews et al., 2014) effectively eliminates the issue, but has disadvantages of complexity and cost. Simplified drying of the sample air combined with humidifying the calibration gas using a permeation water exchanger is a good compromise, with errors of less than 1 ppb CH_4 and even lower for experimentally-determined analyzer-specific correction. It is important to use fits based on the range of low water vapor values, however, or fit the data with a third-order polynomial. Another option, stabilizing the water vapor in both the sample air and calibration gas to minimize the difference between the two (Version 1 described in Liu et al., 2026) may be necessary if the spectrum is locked to the wavelength of a water vapor absorption peak. This method can be used to achieve differences of less than 300 ppm H_2O between sample air and calibration gas. Thus, even relying on the manufacturer's water correction, the error can be low, depending on changes in the ambient temperature (because permeation drier efficiency is temperature dependent) during

https://doi.org/10.5194/egusphere-2026-3732
Preprint. Discussion started: 14 July 2026

the calibration cycle versus during the sample, and thus the frequency of calibration. This effect could be reduced by stabilizing the temperature of the permeation water exchanger, but this complication means that drying the sample air and humidifying the calibration gas may be the best option as long as the analyzer does not require humid air streams.

The current results suggest two improvements for future Aeris CH_4/C_2H_6 networks. Liu et al. (2026) assumed uncertainty for ethane based on the analyzer with the largest water vapor dependence, but noted the difficulty in distinguishing between noise and errors due to water vapor with the testing method utilized. Based on the results of this study, that approach was likely too cautious and the uncertainty of ethane should be based on only noise. In addition, the uncertainties for CH_4 noted in Liu et al. (2026) can be reduced by applying experimentally-determined analyzer-specific water corrections, rather than relying on the manufacturer correction and determining the uncertainty based on the range of measured errors.

The same options for managing water vapor effects exist for the Picarro analyzers, but the relative errors are much reduced compared to compatibility goals (Table 4). Rella et al., (2013) suggested that the manufacturer-supplied water vapor correction was adequate for maintaining CO_2 and CH_4 WMO/GAW compatibility goals for H_2O below 2% for Picarro analyzers without drying the sample air. In this study, the manufacturer-corrected CH_4 bias due to water vapor effects was just within the WMO/GAW compatibility goal for methane at 2 ppb for the tested H_2O range up to 1.7%. However, the manufacturer-corrected CO_2 bias in this study frequently exceeded the ± 0.1 ppm compatibility goal for the three tested Picarro analyzers, exhibiting systematic residual humidity dependence of up to 0.25 ppm. Water vapor levels in the atmosphere frequently are up to 3% or more, however, leading to errors of up to 0.5 ppm CO_2 and 4 ppb CH_4 during periods of high humidity if reliant on manufacturer-provided corrections and not equilibrating the water vapor mole fraction between sample and calibration gases. When maintaining the water vapor mole fraction difference between sample air and calibration gases of less than 0.2% (Richardson et al., 2017) by drying the sample air and humidifying the calibration gas, the corresponding residual errors are low, about 0.03 ppm CO_2 and 0.2 ppb CH_4 even when analyzer-specific experimentally-determined corrections are not applied. With these corrections, the bias is eliminated. The errors for CO are larger relative to desired compatibility, if using ambient air, partially because the manufacturer does not provide a water-corrected value for CO. This study showed that without analyzer-specific water correction for CO, the mean CO bias reached about 12 ppb for the CFKADS2025 and CFKADS2218 analyzers for up to 1.7% H_2O, corresponding to 22 ppb bias for 3% H_2O if a linear dependence is assumed. With equilibration of the water vapor to within 0.2% difference between sample air and calibration gas, this bias is very low, 1.2 ppb. Stabilizing the water vapor of the sample air and calibration gas to be near ambient is also possible, with the drawbacks mentioned previously and no obvious benefits. Experimental determination of analyzer-specific water vapor corrections is a viable alternative to drying or stabilizing the water vapor for achieving the compatibility necessary for many applications. Although time-dependent changes (for periods longer than one month) in instrument-specific water vapor corrections were not addressed in this study, the P-WAVES system developed in this study is well suited for performing routine water vapor correction tests in the field using the calibration cylinder during regular maintenance or site visits.

Table 3: Expected limit of errors due to water vapor calibration for Aeris MIRA Ultra analyzers for different water vapor handling strategies, based on the instruments tested in this manuscript. Typical values for water vapor mole fraction are listed in the description of each option. Drift in the water calibration is not considered. Values are reported as manufacturer-supplied correction

https://doi.org/10.5194/egusphere-2026-3732
Preprint. Discussion started: 14 July 2026

(M) and experimentally determined correction (E). Advantages and disadvantages of each approach are noted. [a]Using a chiller and permeation exchanger (Andrews et al., 2014). [b]Using a permeation water exchanger. [c]Need to determine experimental correction specifically for low water vapor values. [d]Using multiple permeation water exchangers and a mass flow controller.

Option	Aeris CH_4 (ppb, M/E)	Notes
[a]Completely dried sample (100 ppm H_2O) and dry calibration gas (1-2 ppm H_2O)	≈0 / ≈0	Advantage: No need to develop water vapor correction. Disadvantage: Complexity and cost.
[b]Dried sample (1000 ppm H_2O) and humidified calibration gas (500 ppm H_2O)	1 / ≈0[c]	Advantage: Reduced dependence on water vapor correction. Disadvantage: Pump needed for permeation water exchanger, leaks possible. Need analyzer to lock on CH_4 peak, not that of H_2O.
Ambient sample (3% H_2O) and dry calibration gas (1-2 ppm H_2O)	30 / 6	Advantage: No drying system used. Disadvantage: Relatively large errors due to water vapor.
[d]Stabilized sample H_2O (3%) and humidified calibration gas (within 300 ppm of sample is possible)	variable / ≈0	Advantage: No pump needed, unlike drying. Less likelihood of leaks. Disadvantage: Temperature controls the range of water vapor, and this effect may be large depending on temperature control and frequency of calibration.

Table 4: As for Table 3, but for Picarro analyzers. [a]Using a chiller and permeation exchanger (Andrews et al., 2014). [b]Using a permeation water exchanger. [c]Assuming linear response to 3% H_2O. [d]Using multiple permeation water exchangers and a mass flow controller.

Option	Picarro CO_2 (ppm, M/E)	Picarro CH_4 (ppb, M/E)	Picarro CO (ppb, M/E)
[a]Completely dried sample (100 ppm H_2O) and dry calibration gas (1-2 ppm H_2O)	≈0 / ≈0	≈0 / ≈0	≈0 / ≈0
[b]Dried sample (1000 ppm H_2O) and humidified calibration gas (500 ppm H_2O)	≈0 / ≈0	0.5 / ≈0	1 / ≈0
Ambient sample (3% H_2O) and dry calibration gas (1-2 ppm H_2O)	0.5[c] / ≈0	4[c] / ≈0	22[c] / ≈0
[d]Stabilized sample H_2O (3%) and humidified calibration gas (within 300 ppm of sample is possible)	variable / ≈0	variable / ≈0	variable / ≈0

Accurate characterization of water vapor effects remains a challenging but essential component of high-precision GHG measurements. Generating stable and repeatable humidity conditions across a broad range of H_2O mole fractions has historically limited the frequency and practicality of analyzer-specific water vapor calibrations, particularly for field-deployed analyzers. This study demonstrates that residual biases associated with manufacturer-provided corrections can become significant under varying humidity conditions and may exceed WMO/GAW compatibility goals. The stable and portable P-

https://doi.org/10.5194/egusphere-2026-3732
Preprint. Discussion started: 14 July 2026

WAVES system developed in this study provides a practical approach for performing repeated water vapor calibration tests both in laboratory and field environments without requiring analyzers to be returned to the laboratory. This capability enables more frequent verification of analyzer performance and facilitates improved long-term measurement consistency for GHG monitoring applications.

Data availability. The field data presented in this study are available at the following link: https://doi.org/10.26208/xqz9-5m19 (Liu et al., 2026).

Author Contributions. YL contributed to the lab experiments, data collection, data analysis, and writing of the paper. NLM contributed to the lab experiments' design and setup, reviewing, and editing the paper. SJR contributed to building and improving the P-WAVES system, the lab experiments' design and setup, reviewing, and editing the paper. DM contributed to designing and building the P-WAVES system.

Competing Interests. The authors declare that a provisional patent application related to the P-WAVES system described in this manuscript has been filed by the Pennsylvania State University.

Acknowledgements. We would like to thank researchers at the National Oceanic and Atmospheric Administration Global Monitoring Laboratory (NOAA GML) for helpful discussions. This study is based upon work supported by the Department of Energy under award DEFE0032288.

Financial support. This research has been supported by the Department of Energy under award DEFE0032288.

References

Andrews, A. E., Kofler, J. D., Trudeau, M. E., Williams, J. C., Neff, D. H., Masarie, K. A., Chao, D. Y., Kitzis, D. R., Novelli, P. C., Zhao, C. L., Dlugokencky, E. J., Lang, P. M., Crotwell, M. J., Fischer, M. L., Parker, M. J., Lee, J. T., Baumann, D. D., Desai, A. R., Stanier, C. O., De Wekker, S. F. J., Wolfe, D. E., Munger, J. W., and Tans, P. P.: CO_2, CO, and CH_4 measurements from tall towers in the NOAA Earth System Research Laboratory's Global Greenhouse Gas Reference Network: instrumentation, uncertainty analysis, and recommendations for future high-accuracy greenhouse gas monitoring efforts, Atmospheric Meas. Tech., 7, 647–687, https://doi.org/10.5194/amt-7-647-2014, 2014.

https://doi.org/10.5194/egusphere-2026-3732
Preprint. Discussion started: 14 July 2026

Chen, H., Winderlich, J., Gerbig, C., Hoefer, A., Rella, C. W., Crosson, E. R., Van Pelt, A. D., Steinbach, J., Kolle, O., Beck, V., Daube, B. C., Gottlieb, E. W., Chow, V. Y., Santoni, G. W., and Wofsy, S. C.: High-accuracy continuous airborne measurements of greenhouse gases (CO_2 and CH_4) using the cavity ring-down spectroscopy (CRDS) technique, Atmospheric Meas. Tech., 3, 375–386, https://doi.org/10.5194/amt-3-375-2010, 2010.

Chiou, J. S. and Paul, D. R.: Gas permeation in a dry Nafion membrane, Ind. Eng. Chem. Res., 27, 2161–2164, https://doi.org/10.1021/ie00083a034, 1988.

Filges, A., Gerbig, C., Chen, H., Franke, H., Klaus, C., and Jordan, A.: The IAGOS-core greenhouse gas package: a measurement system for continuous airborne observations of CO2, CH4, H2O and CO, Tellus B Chem. Phys. Meteorol., 67, 27989, https://doi.org/10.3402/tellusb.v67.27989, 2015.

Hazan, L., Tarniewicz, J., Ramonet, M., Laurent, O., and Abbaris, A.: Automatic processing of atmospheric CO_2 and CH_4 mole fractions at the ICOS Atmosphere Thematic Centre, Atmospheric Meas. Tech., 9, 4719–4736, https://doi.org/10.5194/amt-9-4719-2016, 2016.

Karion, A., Sweeney, C., Wolter, S., Newberger, T., Chen, H., Andrews, A., Kofler, J., Neff, D., and Tans, P.: Long-term greenhouse gas measurements from aircraft, Atmospheric Meas. Tech., 6, 511–526, https://doi.org/10.5194/amt-6-511-2013, 2013.

Liu, Y., Miles, N. L., Richardson, S. J., Barkley, Z. R., Miller, D. O., Kofler, J., Handley, P., DeVogel, S., and Davis, K. J.: Laboratory and field assessment of mid-infrared absorption (MIRA) instrument performance for methane and ethane dry mole fractions, Atmospheric Meas. Tech., 19, 965–981, https://doi.org/10.5194/amt-19-965-2026, 2026.

Morgan, E. J., Lavrič, J. V., Seifert, T., Chicoine, T., Day, A., Gomez, J., Logan, R., Sack, J., Shuuya, T., Uushona, E. G., Vincent, K., Schultz, U., Brunke, E.-G., Labuschagne, C., Thompson, R. L., Schmidt, S., Manning, A. C., and Heimann, M.: Continuous measurements of greenhouse gases and atmospheric oxygen at the Namib Desert Atmospheric Observatory, Atmospheric Meas. Tech., 8, 2233–2250, https://doi.org/10.5194/amt-8-2233-2015, 2015.

Naudy, S., Collette, F., Thominette, F., Gebel, G., and Espuche, E.: Influence of hygrothermal aging on the gas and water transport properties of Nafion® membranes, J. Membr. Sci., 451, 293–304, https://doi.org/10.1016/j.memsci.2013.10.013, 2014.

Rella, C. W., Chen, H., Andrews, A. E., Filges, A., Gerbig, C., Hatakka, J., Karion, A., Miles, N. L., Richardson, S. J., Steinbacher, M., Sweeney, C., Wastine, B., and Zellweger, C.: High accuracy measurements of dry mole fractions of carbon dioxide and methane in humid air, Atmospheric Meas. Tech., 6, 837–860, https://doi.org/10.5194/amt-6-837-2013, 2013.

Reum, F., Gerbig, C., Lavric, J. V., Rella, C. W., and Göckede, M.: Correcting atmospheric CO_2 and CH_4 mole fractions obtained with Picarro analyzers for sensitivity of cavity pressure to water vapor, Atmospheric Meas. Tech., 12, 1013–1027, https://doi.org/10.5194/amt-12-1013-2019, 2019.

Richardson, S. J., Miles, N. L., Davis, K. J., Lauvaux, T., Martins, D. K., Turnbull, J. C., McKain, K., Sweeney, C., and Cambaliza, M. O. L.: Tower measurement network of in-situ CO2, CH4, and CO in support of the Indianapolis FLUX (INFLUX) Experiment, Elem. Sci. Anthr., 5, 59, https://doi.org/10.1525/elementa.140, 2017.

Stavert, A. R., O'Doherty, S., Stanley, K., Young, D., Manning, A. J., Lunt, M. F., Rennick, C., and Arnold, T.: UK greenhouse gas measurements at two new tall towers for aiding emissions verification, Atmospheric Meas. Tech., 12, 4495–4518, https://doi.org/10.5194/amt-12-4495-2019, 2019.

https://doi.org/10.5194/egusphere-2026-3732
Preprint. Discussion started: 14 July 2026

Welp, L. R., Keeling, R. F., Weiss, R. F., Paplawsky, W., and Heckman, S.: Design and performance of a Nafion dryer for continuous operation at CO_2 and CH_4 air monitoring sites, Atmospheric Meas. Tech., 6, 1217–1226, https://doi.org/10.5194/amt-6-1217-2013, 2013.

Zellweger, C., Steinbacher, M., Brailsford, G., Laurent, O., Crotwell, A., Jordan, A., Krummel, P., Lan, X., Loh, Z., Mund, J., Tarasova, O., Tsuboi, K., and Vermeulen, A.: Measurement Guidelines for the Observations of CO_2, CH_4 and N_2O at Global Atmosphere Watch Stations, GAW Report No. 316, World Meteorological Organization, Geneva, Switzerland, 2025.